Research Article

Journal of Environmental Nanotechnology

Carbon Nanotube-based Detection of Cancer-related Biomarkers (Methyl Mercaptan, Benzene and Aniline): A First-principles Approach

Kirtesh Pratap Khare[1*] and Anurag Srivastava[2]

[1]Department of Biosciences, Acropolis Institute of Management Studies and Research, Indore, MP, India
[2]Advanced Materials Research Group, Materials Synthesis and Sensor Design Laboratory, ABV-Indian Institute of Information Technology and Management, Gwalior, MP, India
Received: 05.10.2025 Accepted: 15.11.2025 Published: 30.12.2025
*kirteshpratapkhare@acropolis.edu.in

ABSTRACT

Cancer is a complex disease caused by genetic changes, and its early detection is essential for effective treatment and reduced mortality. Biomarkers play a key role in cancer diagnosis and prognosis. In this study, a pristine carbon nanotube (CNT) is proposed as a sensor for detecting cancer-related biomarkers such as methyl mercaptan, benzene, and aniline. The sensing performance is investigated using Density Functional Theory (DFT) with the Quantum ATK method by analyzing band gap, density of states, adsorption energy, charge transfer, recovery time, conductance, and sensitivity. The negative adsorption energy values confirm stable physical adsorption, indicating low operating temperature and good reusability. The results demonstrate that pristine CNT shows good stability and sensitivity toward the target molecules, highlighting its potential for early cancer biomarker detection.

Keywords: Carbon nanotubes; Density functional theory; Cancer biomarkers; Recovery time; Conductance; Sensitivity.

1. INTRODUCTION

Cancer is a common cause of mortality worldwide (Doll *et al*. 2004; Yang *et al.* 2004; You *et al.* 2015; World Health Organization 2005). Early detection and treatment of the disease improve the chances of cancer cure (Wulfkuhle *et al*. 2003; Talmadge and Fidler 2010; Oppenheimer 2006). Methods for anticipating cancer therapies have advanced (Neskey *et al*. 2015; Milosevic *et al*. 2018; Kourou *et al*. 2015; Khoury *et al*. 2013; Ramasamy and Nirmala, 2020). A biomarker is a physiologically significant intra- or intercellular molecule whose expression or activity is either responsible for the associated clinical circumstances or is specifically altered in response to them (Valko *et al*. 2007). Proteins on the surface of cancer cells present in blood and serum are examples of biomarkers of cancer that aid in diagnosis (Perfézou *et al*. 2012; Kosaka *et al.* 2010). Extensive research is necessary to detect biomarkers at extremely low concentrations (Campuzano *et al*. 2017; Bu *et al*. 2014). Reduced sulfur compounds (RSCs), benzene, and aniline have a major effect on worldwide atmospheric composition and play a major part in the formation of atmospheric aerosols (Bordbar *et al*. 2020). Natural (resulting from the decrease of phosphate in aerobic fluids and soils) and anthropomorphic (derived from burning fossil fuel, petrochemical sector or public waste water structures) sources introduce them into the environment (Niele 2005). The design of an effective surveillance technique to detect such contaminant is therefore a significant issue for the safety of the environment (Pratap *et al*. 2021; Li *et al*. 2019**).** In addition to their environmental relevance, CH_4S, C_6H_6, and C_6H_7N have been reported to originate from altered metabolic pathways, oxidative stress, and abnormal enzymatic activity in cancerous tissues, and are frequently detected as volatile organic compounds (VOCs) in the exhaled breath and biological samples of cancer patients, thereby establishing their relevance as cancer-related metabolic biomarkers. For industrial purposes, the great advantage of mercaptan is that it can be detected in extremely small quantities, less than one part per million (Srivastava, 2012). Carbon nanotubes are 1D allotropes of carbon. Carbon nanotube shows the unique properties due to their cylindrical framework, excellent mechanical strength and detecting power toward poisonous gases (Erol *et al*. 2018; Jeon *et al*. 2011; Terrones 2004). Their high surface-to-volume ratio, tunable electronic properties, and strong interaction with VOC molecules make CNTs uniquely suited for detecting trace-level cancer-related gases. However, many previously reported CNT-based sensors suffer from limitations such as poor selectivity, slow recovery time, or the need for surface functionalization and high operating temperatures. The sensing mechanism of pristine CNT is based on the adsorption of target gas molecules on its surface, which induces charge transfer between the analyte molecules and the CNT, leading to a

change in its electronic structure and electrical conductivity. Such changes in conductance act as the sensing signal for the detection of specific molecules. In this work we used pristine CNT as a cancer biomarker for the detection of CH_4S, C_6H_6, and C_6H_7N molecule.

2. COMPUTATIONAL DETAILS

For the sensing behavior of pristine CNT towards CH_4S, C_6H_6, and C_6H_7N has been adjudged using quantum ATK method (Pratap *et al*. 2021), a Density Functional Theory (Capelle 2006) based *ab initio* approach. Since quantum ATK uses the same basis sets as SIESTA, it improves TranSIESTA's, accuracy. Using the Generalized Gradient Approximation (GGA) as the exchange-correlation functional, the Perdew-Burke-Ernzerhof (PBE) geometry optimization of the projected assembly of the system has been applied to find the electrical properties (Agrawal *et al*. 2021). Double zeta double polarization (DZDP) basis sets are considered to represent various electronic states. A mesh cut off of 75 Rydberg has been found sufficient for the improved electron density on a regular real-space grid. Brillouin zone sampling was performed using a Monkhorst–Pack k-point grid of 1 × 1 × 10, appropriate for the one-dimensional nature of the CNT system. Different possible configurations have been attempted and optimized to confine the structure of pristine CNT in the presence of CH_4S, C_6H_6, and C_6H_7N. The maximum force and maximum stress tolerance during geometry optimization have been set at 0.05 eV/Å^3 and 0.05 eV/Å, respectively.

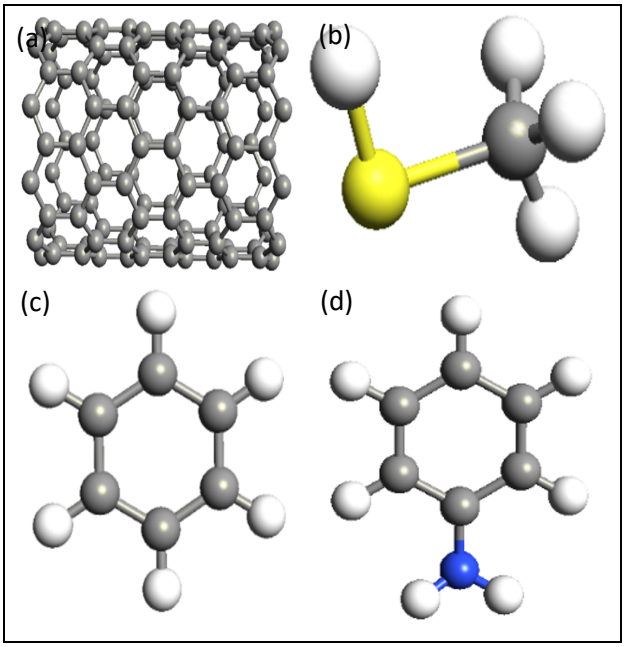


Fig. 1: (a-d) Optimized geometries of (a) Pristine CNT, (b) CH_4S, (c) C_6H_6 and (d) C_6H_7N

3. RESULTS AND DISCUSSION

3.1 Structural Stability

The optimal geometries of pristine CNT, as displayed in Fig. 1 and 2 are in the absence/presence of CH_4S, C_6H_6, and C_6H_7N molecules. Table 1 reports the total energy of the optimized geometries in structural and stability analysis. The optimized distances (Å) between the CNT surface and CH_4S, C_6H_6, and C_6H_7N molecules are found to be 3.03, 3.61, and 3.55 Å, respectively. The value of total energy indicates the pristine CNT in the presence of CH_4S, C_6H_6, and C_6H_7N molecules is minimum in comparison to their absence. The computed total energy confirms that the pristine CNT shows the better stability in the presence of CH_4S, C_6H_6, and C_6H_7N molecules in comparison to their absence.

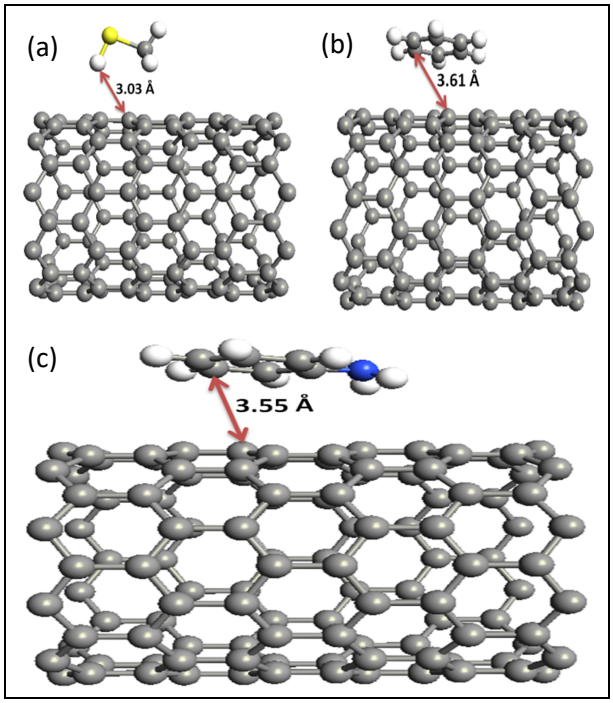


Fig. 2 (a-c) Optimized geometries of Pristine CNT with adsorbed (a) CH_4S, (b) C_6H_6, and (c) C_6H_7N molecules

3.2 Electronic Properties

Table 1. Total energy of pristine CNT in the absence/presence of CH_4S, C_6H_6, and C_6H_7N

System	Total energy (eV)
CNT	-18883.79
CNT_CH_4S	-19463.61
CNT_C_6H_6	-19924.11
CNT_C_6H_7N	-20211.94

In order to comprehend the electronic characteristics of pristine CNT in the absence/presence of

CH_4S, C_6H_6, and C_6H_7N molecules, band gap has been computed. When a single molecule of CH_4S, C_6H_6, and C_6H_7N is brought in vicinity of the surface of pristine CNT, the band gap changed. This was confirmed through the band structure profile represented in Fig. 3 (a-d). The variation in band gap reflects the interaction between the adsorbed molecules and the CNT surface, leading to modification in its electronic structure, which is crucial for sensing applications as it directly influences conductivity. Band gap of pristine CNT in the presence of CH_4S, C_6H_6, and C_6H_7N molecules has been computed and compared with pristine CNT. The computed band gap of pristine CNT in the absence of CH_4S, C_6H_6, and C_6H_7N molecules is 0.72 eV, whereas the band gap of the same sets in the presence of CH_4S, C_6H_6, and C_6H_7N molecules has been reduced to 0.71 eV, 0.70 eV, and 0.71 eV, respectively, as reported in Table 2. The larger reduction in band gap observed for C_6H_6 is due to its stronger π–π interaction with the CNT surface, which facilitates greater charge transfer compared to CH_4S, thereby more effectively altering the electronic structure of CNT.

In addition, to understand the variation in electronic properties of pristine CNT in the absence/presence of CH_4S, C_6H_6, and C_6H_7N molecules, density of state (DOS) profile has also been computed, as depicted in Fig. 3 (a-d). DOS profile of pristine CNT in the presence of CH_4S, C_6H_6, and C_6H_7N molecules has altered. During the interaction between adsorbate and adsorbent, the Fermi level shifts towards balance/conduction band and few extra peaks appeared and the length of peaks have also been altered in the valence as well as conduction band as shown in Fig. 3 (a-d).

Table 2. Band gap, conductance, sensitivity, and charge transfer for adsorbing system

System	Band-gap (eV)	Conductance (S)	Sensitivity (%)	QT (e)
CNT	0.72	5.458e-10	-	-
CNT_CH_4S	0.71	1.162e-10	78.71	0.061
CNT_C_6H_6	0.70	1.162e-10	78.71	0.003
CNT_C_6H_7N	0.71	1.162e-10	78.71	0.004

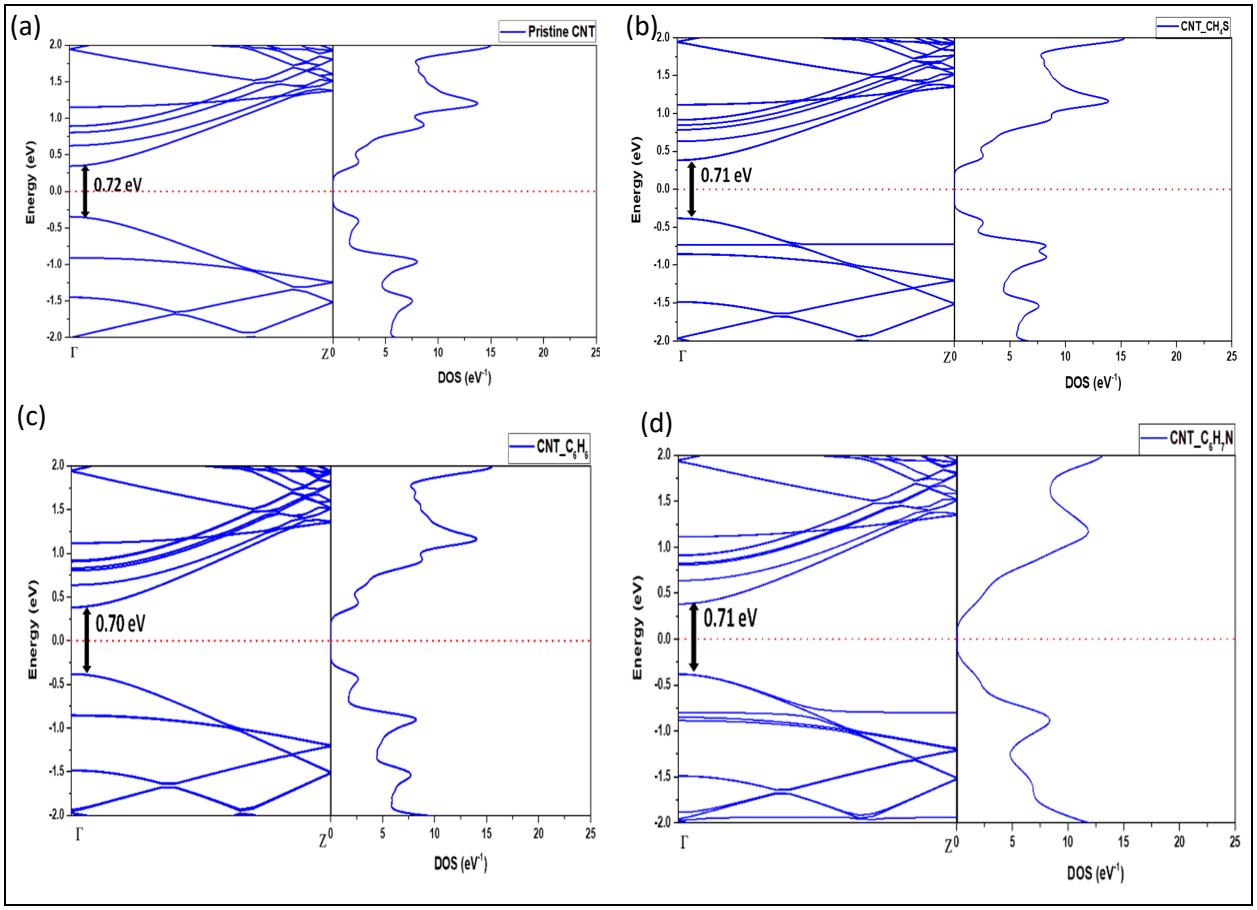


Fig. 3 (a-d) Electronic band structure and DOS profiles of (a) Pristine CNT with adsorbed (b) CH_4S, (c) C_6H_6 , and (d) C_6H_7N molecules

3.3 Adsorption Energy

To comprehend the interaction between pristine CNT and CH_4S, C_6H_6, and C_6H_7N molecules, adsorption energy is a crucial metric. In the present work we have calculated the adsorption energy with the help of the following equation. The calculated adsorption energy is negative in all cases (Table 3).

$$E_{ads} = ET_{(optimized\ system)} - ET_{(pristine\ CNT)} - ET_{(molecules)}, \quad \ldots (1)$$

where ET (Optimized system) is the total energy of the optimized system post adsorption, ET (pristine CNT) is the total energy of optimized pristine CNT, and ET (molecules) is the total energy of optimized CH_4S, C_6H_6, and C_6H_7N molecules. In every instance, physical adsorption and an exothermic interaction between the adsorbent and adsorbate are indicated by negative adsorption energy, confirming the stability and strength of the adsorption system. The adsorption energy in case of pristine CNT in the presence of CH_4S molecule is the minimum and in case of pristine CNT in the presence of C_6H_7N molecule is maximum. The inference of physical adsorption energy is also verified by optimized geometries, as shown in Fig. 2 (a-c). They denote that no chemical bond formed between pristine CNT and CH_4S, C_6H_6, and C_6H_7N molecules.

To understand the interaction between pristine CNT and CH_4S, C_6H_6, and C_6H_7N molecules, recovery time (τ), as a function of adsorption energy (E_{ads}) in the following equation.

$$(\tau) = \upsilon^{-1}\exp(-E_{ads}/K_bT), \quad \ldots (2)$$

where, (υ) is the attempt frequency, (K_b) the Boltzmann constant and (T) is operational temperature. Adsorption energy (E_{ads}) and recovery time (τ) are inversely proportional. The adsorption energy shows the trend: CNT_C_6H_7N > CNT_C_6H_6 > CNT_CH_4S and the recovery time shows the trend CNT_C_6H_7N < CNT_C_6H_6 < CNT_CH_4S. Recovery time of pristine CNT in the presence of CH_4S molecule is fast with less operational temperature in comparison to other adsorbed systems.

Table 3. Optimized distance and Adsorption energy of CH_4S, C_6H_6, and C_6H_7N adsorbed system.

System	Optimized Distance (Å)	Adsorption Energy (eV)	Type of Interaction
CNT_CH_4S	3.03	-0.32	Physisorption
CNT_C_6H_6	3.61	-0.50	Physisorption
CNT_C_6H_7N	3.55	-0.61	Physisorption

3.4 Charge Transfer Analysis

The charge transfer parameters have been calculated using Mulliken population analysis as shown in Table 2. It paves way to fully comprehend the interaction between pristine CH_4S, C_6H_6, and C_6H_7N molecules. The negative values of charge transfer indicate the charge transfers from adsorbate to adsorbent and the positive value indicate the reverse. In the present work, the charge transfers from pristine CNT to CH_4S, C_6H_6, and C_6H_7N molecules. The charge transfers values in pristine CNT with CH_4S, C_6H_6, and C_6H_7N molecules, shows the following trends pristine CNT_CH_4S (0.061) > pristine CNT_C_6H_7N (0.004) > pristine CNT_C_6H_6 (0.003) The higher charge transfer observed for CH_4S is attributed to its stronger electronic interaction and higher electron-donating capability, which facilitates more effective electron exchange with the CNT surface.

3.5 Range of detection Analysis

The adsorption mechanism of pristine CNT with CH_4S, C_6H_6, and C_6H_7N molecules has been analyzed in terms of the detection range, shown in Table 3. Fig. 4 clarifies the variation of conductance as a function of distance of the CH_4S, C_6H_6, and C_6H_7N molecules from pristine CNT within the optimized distance. It demonstrates inverse relationship with distance between pristine CNT and CH_4S, C_6H_6, and C_6H_7N molecules and the conductance. In case of CH_4S and C_6H_7N molecules, conductance decreases up to a certain distance and then constant. In case of C_6H_6 adsorbed pristine CNT, the conductance decreases up to a certain distance (2.5 Å), after which it increases. This confirms the sensitivity of pristine CNT for CH_4S, C_6H_6, and C_6H_7N molecules. The computed zero bias conductance for the pristine CNT is found be 5.458e-10 and after adsorption of CH_4S, C_6H_6, and C_6H_7N molecules, it is 1.162e-10, 1.162e-10, and 1.162e-10. The equation given below and Table 2 reflect the results of this analysis of the computed conductance, it was additionally employed to test the sensitivity of pure CNT for CH_4S, C_6H_6, and C_6H_7N molecules.

$$\mathbf{S = G - G_o/G}, \quad \ldots (3)$$

where G_o is the conductance of pristine CNT and G is the conductance of CH_4S, C_6H_6, and C_6H_7N adsorbed system. The sensitivity, estimated as a function of conductance, is 78.71 % in pristine CNT adsorbed CH_4S, C_6H_6, and C_6H_7N molecules. These findings confirm that the sensitivity for CH_4S, C_6H_6, and C_6H_7N molecules with pristine CNT is same. The obtained conductance variation and sensitivity values are consistent with previously reported experimental CNT-based VOC sensors, where adsorption-induced charge transfer leads to comparable changes in electrical response, thereby

supporting the practical relevance of the present theoretical results.

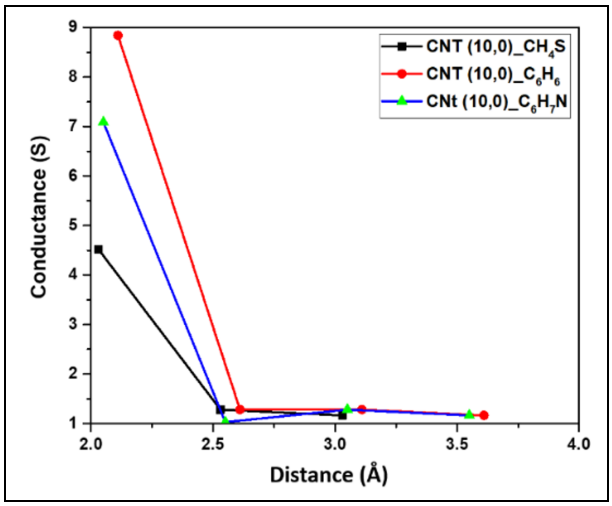


Fig. 4 Distance *vs.* Conductance analysis of CNT with adsorbed CH4S, C6H6, and C6H7N molecules

3.6 Current-Voltage Analysis

By expanding the scattering zone of the pristine CNT as the left and right electrodes, a two-probe model was used to determine the current-voltage at zero bias in the presence of CH_4S, C_6H_6, and C_6H_7N molecules, shown in Fig. 5 (a-c). Fig. 6 shows the current-voltage characteristics of pristine CNT in the absence/presence of CH_4S, C_6H_6, and C_6H_7N molecules. The highest current has been recorded in the event where C_6H_6 molecule adsorbed pristine CNT after an applied voltage of 0.3 V. Minimum current has been observed in case of pristine CNT after an applied voltage of 0.6 V in comparison to other adsorbed systems. In case of CH_4S adsorbed pristine CNT, the current increases after an applied voltage of 0.5 V and for C_6H_7N adsorbed pristine CNT, the current increases after an applied voltage above 0.5 V, and below this voltage, small current is observed. The higher current observed for C_6H_6 at 0.3 V can be attributed to its stronger π–π interaction and more efficient charge transfer with the CNT, which enhances electron mobility along the nanotube. As the variation in the current voltage characteristics at varying voltage are clearly distinct (Fig. 6), the variation in the I-V characteristics also validates the sensitivity of pristine CNT towards considered CH_4S, C_6H_6, and C_6H_7N molecules. These distinct I–V responses imply that pristine CNT can effectively discriminate between different VOCs in real sensor circuits, offering potential for selective and sensitive detection at low operating voltages.

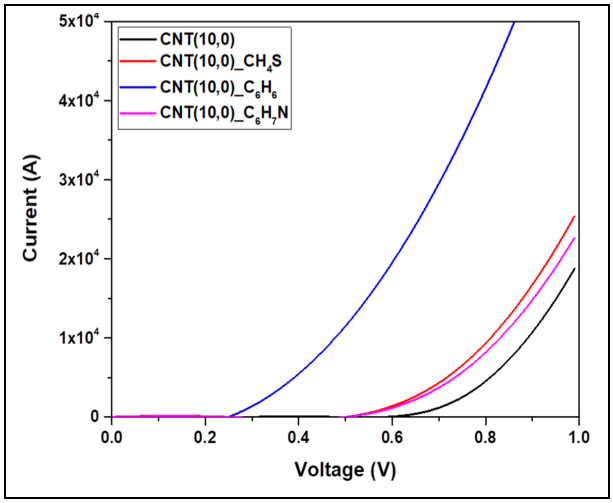


Fig. 6. I-V analysis of CNT with adsorbed CH_4S, C_6H_6, and C_6H_7N molecules

4. CONCLUSION

This study presents a DFT-based simulation of pristine carbon nanotubes as detectors for CH_4S, C_6H_6, and C_6H_7N cancer biomarkers. Electronic characteristics and current-voltage analysis confirm that these molecules can be sensed *via* noticeable changes in the properties of CNT. The results show that CNTs exhibit better stability in the presence of the target molecules, and their physical adsorption ensures reusability at low operating temperatures. CH_4S adsorbed CNT shows faster recovery, while C_6H_6 adsorbed CNT demonstrates a wider detection range and maximum current. Future work may focus on CNT functionalization, experimental validation, and sensor miniaturization for practical biomedical applications.

ACKNOWLEDGEMENTS

The authors are grateful to the Advanced Materials Research Group of Carbon Nano Laboratory, ABV-IIITM, Gwalior for providing the computational resources and access to the e-library for the present research work.

FUNDING

The authors declare that no funds, grants, or other support were received during the preparation of this manuscript.

CONFLICTS OF INTEREST

The authors declare that there is no conflict of interest.

COPYRIGHT

This article is an open-access article distributed under the terms and conditions of the Creative Commons Attribution (CC BY) license (http://creativecommons.org/licenses/by/4.0/).



REFERENCES

Agrawal, S., Kaushal, G. and Srivastava, A., Electron transport in C_3N monolayer: DFT analysis of volatile organic compound sensing, *Chem. Phys. Lett.,* 762, 138121 (2021). https://doi.org/10.1016/j.cplett.2020.138121

Bordbar, M. M., Nguyen, T.-A., Tran, A. Q. and Bagheri, H., Optoelectronic nose based on an origami paper sensor for selective detection of pesticide aerosols, *Sci. Rep.,* 10(1), 1–12 (2020). https://doi.org/10.1038/s41598-020-74509-8

Bu, L., Shen, B. and Cheng, Z., Fluorescent imaging of cancerous tissues for targeted surgery, *Adv. Drug Deliv. Rev.,* 76, 21–38 (2014). https://doi.org/10.1016/j.addr.2014.07.008

Campuzano, S., Yáñez-Sedeño, P. and Pingarrón, J. M., Electrochemical bioaffinity sensors for salivary biomarkers detection, *TrAC Trends Anal. Chem*., 86, 14–24 (2017). https://doi.org/10.1016/j.trac.2016.10.002

Capelle, K., A bird's-eye view of density-functional theory, *Braz. J. Phys.,* 36(4A), 1318–1343 (2006). https://doi.org/10.1590/S0103-73320060000700035

Doll, R., Peto, R., Boreham, J. and Sutherland, I., Mortality in relation to smoking: 50 years' observations on male British doctors, *BMJ*, 328(7455), 1519 (2004). https://doi.org/10.1136/bmj.38142.554479.AE

Erol, O., Uyan, I., Hatip, M., Yilmaz, C., Tekinay, A. B. and Guler, M. O., Recent advances in bioactive 1D and 2D carbon nanomaterials for biomedical applications, *Nanomed. Nanotechnol. Biol. Med*., 14(7), 2433–2454 (2018). https://doi.org/10.1016/j.nano.2018.06.015

F. Niele, Energy: Engine of Evolution. Elsevier, 2005. ISBN-13: 9780444518866

Jeon, I. Y., Chang, D. W., Kumar, N. A. and Baek, J. B., Functionalization of carbon nanotubes, *Carbon Nanotub. Nanocompos.,* 91–110 (2011). https://doi.org/10.5772/18396

Khoury, M. J., Lam, T. K., John, L. P. A., Hartge, P., Spitz, M. R.,Buring, J. E., Stephen, C. J., Robert, T. C., Katrina, G. A., Geoffrey, S. G., Zdenko, H., Robert, A. H., Hoover, D. J., Kramer, B. S., Lauer, M. S., Jeffrey, A. M., Olopade, O., Palmer, J, R., Sellers, T. A., Seminara, D., Ransohoff, D. F., Rebbeck, T. R., Tourassi, G., Winn, D. M., Ann, Z. and Sheri, S. D., Transforming epidemiology for 21st century medicine and public health, *Cancer Epidemiol. Prev. Biomarkers,* 22(4), 508–516 (2013). https://doi.org/10.1158/1055-9965.EPI-13-0146

Kosaka, N., Iguchi, H. and Ochiya, T., Circulating microRNA in body fluid: a new potential biomarker for cancer diagnosis and prognosis, *Cancer Sci.,* 101(10), 2087–2092 (2010) https://doi.org/10.1111/j.1349-7006.2010.01650.x

Kourou, K., Exarchos, T. P., Exarchos, K. P., Karamouzis, M. V. and Fotiadis, D. I., Machine learning applications in cancer prognosis and prediction, Comput. Struct. Biotechnol. J., 13, 8–17 (2015). https://doi.org/10.1016/j.csbj.2014.11.005

Li, Y., Wang, Z., Sun, L., Liu, L., Xu, C. and Kuang, H., Nanoparticle-based sensors for food contaminants, *TrAC Trends Anal. Chem*., 113, 74–83 (2019). https://doi.org/10.1016/j.trac.2019.01.012

Milosevic, M., Jankovic, D., Milenkovic, A. and Stojanov, D., Early diagnosis and detection of breast cancer, Technol. Health Care, 26(4), 729–759 (2018). https://doi.org/10.3233/THC-181277

Neskey, D. M., Osman, A. A., Ow, T. J., Katsonis, P., Thomas, M., Hicks, S. C., Hsu, T. K., Curtis, P. R., Ward, A., Patel, A., Yordy, J. S., Skinner, H. D., Giri, U., Sano, D., Story, M. D., Beadle, B. M., Adel, E. K., Kies, M. S., William, W. N., Caulin, C., Mitchell, F., Kimmel, M., Myers, J. N. and Olivier, L., Evolutionary action score of TP53 identifies high-risk mutations associated with decreased survival and increased distant metastases in head and neck cancer, *Cancer Res.,* 75(7), 1527–1536 (2015). https://doi.org/10.1158/0008-5472.CAN-14-2735

Oppenheimer, S. B., Cellular basis of cancer metastasis: A review of fundamentals and new advances, *Acta Histochem.,* 108(5), 327–334 (2006). https://doi.org/10.1016/j.acthis.2006.03.008

Perfézou, M., Turner, A. and Merkoçi, A., Cancer detection using nanoparticle-based sensors, *Chem. Soc. Rev*., 41(7), 2606–2622 (2012). https://doi.org/10.1039/C1CS15134G

Pratap, K., Neelima, K. and Srivastava, A., 6-Thioguanine Sensing Using Poly Pyrrole: DFT Study, 17, 1–5, (2021). https://doi.org/10.1063/5.0052388

Ramasamy, S. and Nirmala, K., Disease prediction in data mining using association rule mining and keyword-based clustering algorithms, *Int. J. Comput. Appl.,* 42(1), 1–8 (2020). https://doi.org/10.1080/1206212X.2017.1396415

Srivastava, V. C., An evaluation of desulfurization technologies for sulfur removal from liquid fuels, *RSC Adv.,* 2(3), 759–783 (2012). https://doi.org/10.1039/C1RA00309K

Talmadge, J. E. and Fidler, I. J., AACR centennial series: the biology of cancer metastasis: historical perspective, *Cancer Res.,* 70(14), 5649–5669 (2010). https://doi.org/10.1158/0008-5472

Terrones, M., Carbon nanotubes: synthesis and properties, electronic devices and other emerging applications, *Int. Mater. Rev.,* 49(6), 325–377 (2004). https://doi.org/10.1179/174328004X5655

Valko, M., Leibfritz, D., Moncol, J., Cronin, M. T. D., Mazur, M. and Telser, J., Free radicals and antioxidants in normal physiological functions and human disease, *Int. J. Biochem. Cell Biol.,* 39(1), 44–84, (2007). https://doi.org/10.1016/j.biocel.2006.07.001

World Health Organization, Global action against cancer, 2005. ISBN 9241593148

Wulfkuhle, J. D., Liotta, L. A. and Petricoin, E. F., Proteomic applications for the early detection of cancer, *Nat. Rev. Cancer*, 3(4), 267–275 (2003). https://doi.org/10.1038/nrc1043

Yang, B. H., Bray, F. I., Parkin, D. M., Sellors, J. W. and Zhang, Z., Cervical cancer as a priority for prevention in different world regions: an evaluation using years of life lost, *Int. J. Cancer*, 109(3), 418–424 (2004). https://doi.org/10.1002/ijc.11719

You, D., Hug, L., Simon, E., Idele, P., Higan, D., Colin, M., Gerland, P., New, J. R. and Alkema, L., Global, regional, and national levels and trends in under-5 mortality between 1990 and 2015, with scenario-based projections to 2030: a systematic analysis by the UN Inter-agency Group for Child Mortality Estimation, *Lancet,* 386(10010), 2275–2286 (2015). https://doi.org/10.1016/S0140-6736(15)00120-8